Supplementary Information

Three-dimensional on-chip micromanipulation using bulk acoustic waves

Emilie Vuille-dit-Bille, Marc-Alexandre Dubois, Junsun Hwang, Dara Bayat, Thomas Overstolz, Amit Dolev, Sarah Heub, Gilles Weder, Michel Despont and Mahmut Selman Sakar

Supplementary Figures

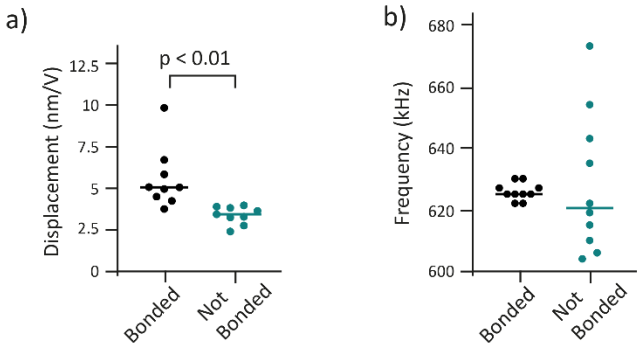

Supplementary Figure 1. Effect of anodic bonding on the vibrational response of the transducers. Comparison between PMUT arrays that are anodically bonded to glass (Bonded) and without anodic bonding (Not Bonded). a) Displacement at the center of the PMUT measured at its fundamental resonance frequency. b) Resonance frequency of the PMUTs. All measurements were done in water on a PMUT array with radius = 450 µm and pitch = 1500 µm.

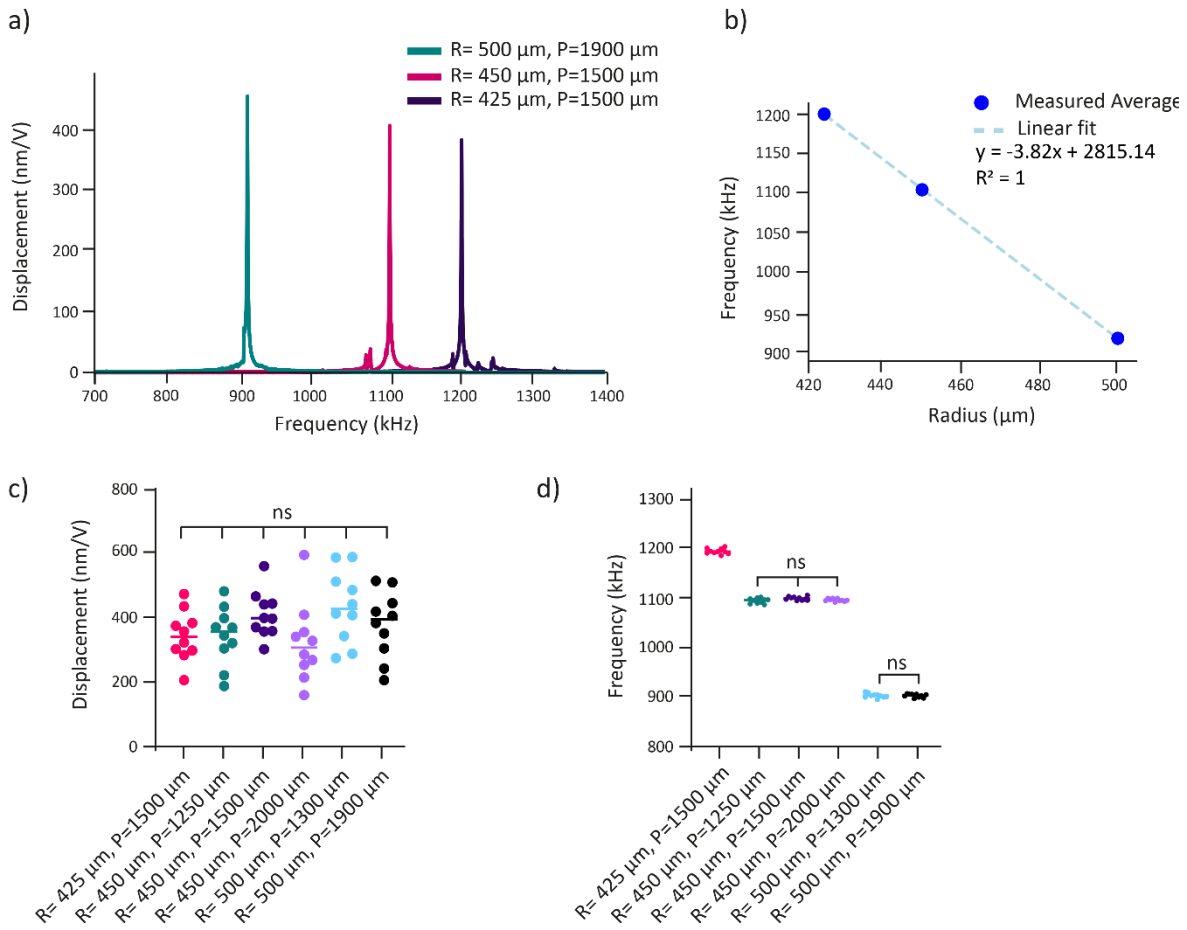

Supplementary Figure 2. Vibrational characterization of PMUTs in air with varied PMUT radius (R) and pitch (P). a) Frequency response of PMUTs with different radii. b) Resonance frequency as a function of PMUT radius. c) Maximal displacement amplitude at the fundamental resonance frequency for various array designs with differing radii and pitches. No statistically significant difference was observed across the designs. d) Resonance frequency of PMUTs for different array designs. Arrays with identical PMUT radii but varying pitch show no statistically significant variation in resonance frequency.

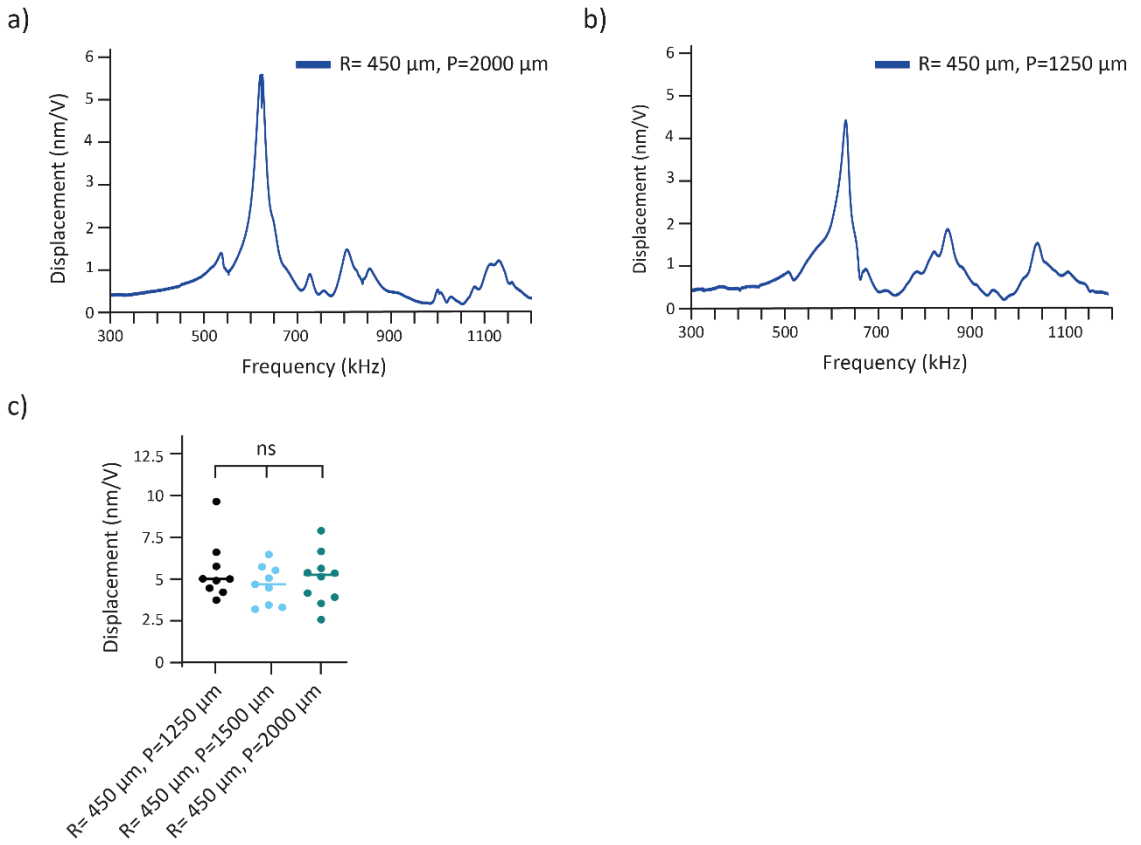

Supplementary Figure 3. Vibrational characterization of PMUTs in water for different array designs with a unique PMUT radius (R: 450 µm) but with varied pitch (P). a-b) Frequency response of a PMUT with different pitches: (a) pitch = 2000 µm and (b) pitch = 1250 µm. c) Maximum displacement at the fundamental resonance frequency for different pitches. There is no statistical difference between all the designs.

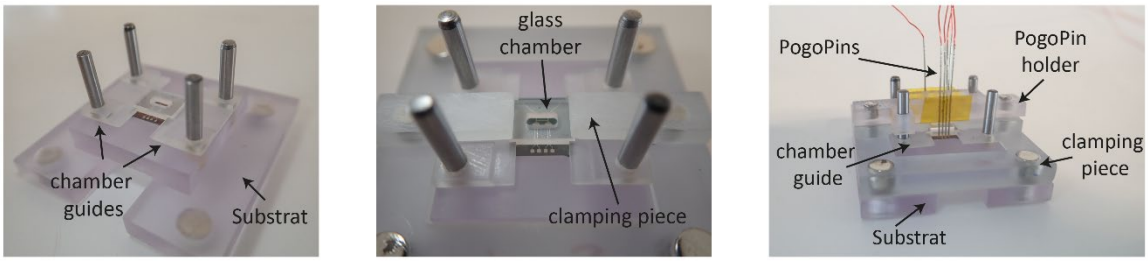

Supplementary Figure 4. Components of the custom clamping setup. Photographs showing the individual components of the custom-designed clamping system used for PMUT array operation. The setup consists of five parts: one substrate, two chamber guides, one clamping piece, and one PogoPin holder. Each component is designed to ensure precise alignment, secure sealing, and reliable electrical interfacing during experimental measurements.

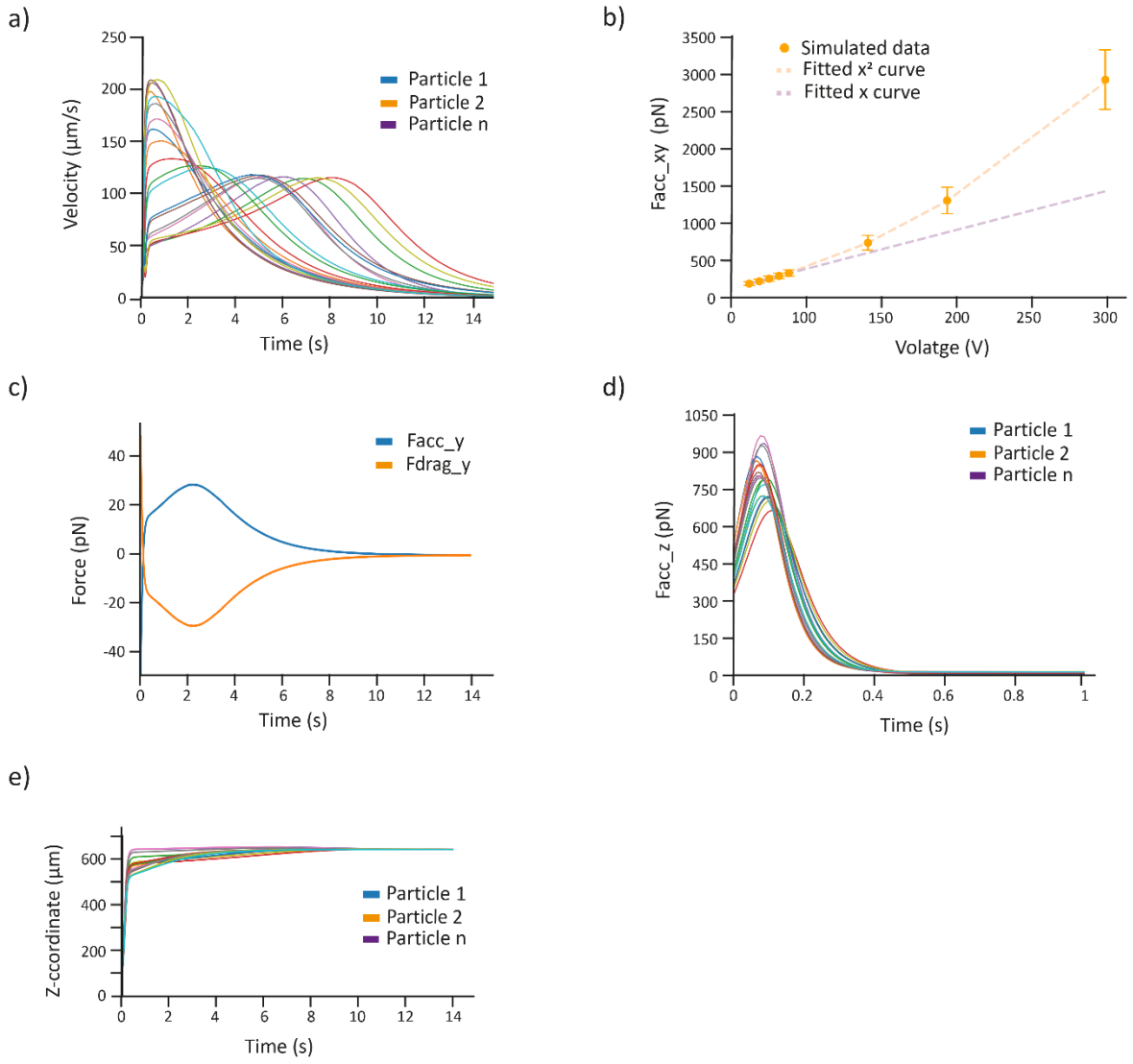

Supplementary Figure 5. Simulated variables describing particle trajectories during acoustic manipulation. a) In-plane velocity as a function of time for 20 particles at 75 V_p excitation. b) Maximum in-plane velocity of particles as a function of applied voltage. Each data point represents the average maximum velocity across 20 particles. The observed trend confirms a quadratic dependence on the excitation voltage. c) Comparison between the in-plane acoustic radiation force and hydrodynamic drag force for a single particle at 75 V_p, highlighting their equivalence. d) Vertical acoustic radiation force for 20 particles during acoustic trapping. e) Time evolution of the z-position for 20 particles, showing vertical localization of the acoustic trap at 75 V_p.

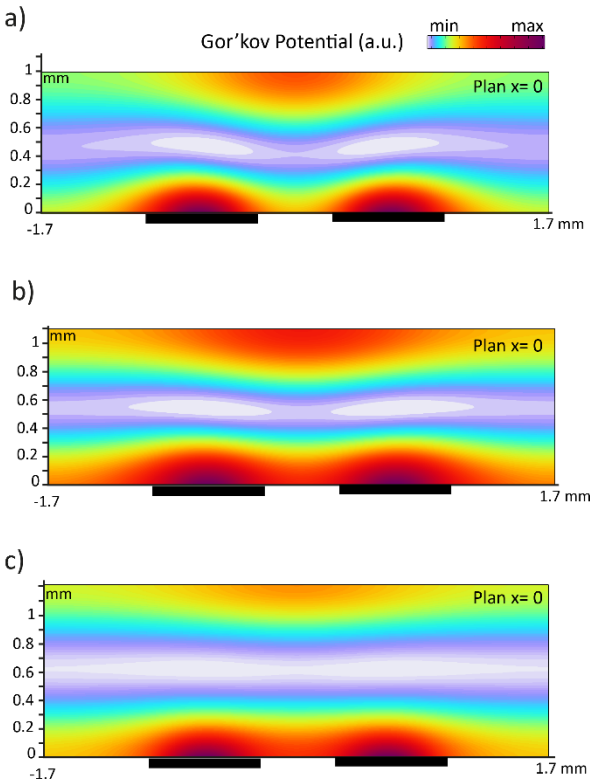

Supplementary Figure 6. Simulated Gor'kov potential for different chamber height. a-c) Gor'kov potential for the vertical cross-section plan x = 0 for (a) h = 1000 µm, (b) h = 1100 µm and (c) h = 1200 µm. Dark rectangles indicate PMUT locations.

Supplementary Table

Table S1 Expression of functions and parameters used in the FE simulation using COMSOL MULTIPHYSICS.

Name	Expression	Unit	Description
U_gor	(f1Gor-f2Gor)	Pa = J/m³	Gor'kov potential energy density
f1Gor	(f1*.5*realdot(acpr.p_t,acpr.p_t))/(2*acpr.rho*c0^2)	Pa= J/m³	
f2Gor	0.75*f2*acpr.rho*.5*(realdot(acpr.vx,acpr.vx)+realdot(acpr.vy,acpr.vy) + realdot(acpr.vz,acpr.vz))	Pa= J/m³	
f1	1-(k_p/k_m)		
f2	2*((rho_p-acpr.rho)/(2*rho_p+acpr.rho))		
rho_p	1100	kg/m³	Density PS particles[1]
c0	1480	m/s	Speed of sound in water[2]
k_p	2.47E-10	Pa	Compressibility PS particles[1]
k_m	4.56E-10	Pa	Compressibility water[2]
cL_p	2350	m/s	Longitudinal (pressure) wave speed PS particles[1]
cT_p	1120	m/s	Transverse (shear) wave speed PS particles[1]

Supplementary Videos

Supplementary video 1: Acoustic trapping of PS particles in PMUT-based platform.

Supplementary video 2: Simulated trajectories of PS particles in PMUT-based platform.

Supplementary video 3: In-plane trajectories of PS particles.

Supplementary video 4: Influence of chamber height: acoustic trapping of PS particles in two traps (h = 1000 μm).

Supplementary video 5: In-flow acoustic trapping of PS particles.

Supplementary video 6: Limits of in-flow acoustic trapping.

Supplementary video 7: Bidirectional translation of PS particles between adjacent PMUTs.

Supplementary video 8: Translation and merging of PS particle aggregates between adjacent PMUTs.

References

1. Settnes, M. & Bruus, H. Forces acting on a small particle in an acoustical field in a viscous fluid. *Phys. Rev. E* **85**, 016327 (2012).
2. Modeling an Acoustic Trap: Thermoacoustic Streaming and Particle Tracing. *COMSOL* https://www.comsol.com/blogs/modeling-an-acoustic-trap-thermoacoustic-streaming-and-particle-tracing.